

# MapFormer: Self-Supervised Learning of Cognitive Maps with *input-dependent* positional encoding

Victor Rambaud<sup>1,2,3</sup> Salvador Mascarenhas<sup>1,3</sup> Yair Lakretz<sup>2,3</sup>

## Abstract

A cognitive map is an internal model which encodes the abstract relationships among entities in the world, giving humans and animals the flexibility to adapt to new situations, with a strong out-of-distribution (OOD) generalization that current AI systems still do not possess. To bridge this gap, we introduce *MapFormers*, new architectures based on Transformer models, which can learn cognitive maps from observational data and perform path integration in parallel, in a self-supervised manner. Cognitive maps are learned in the model by disentangling structural relationships in the inputs from their specific content, a property that can be achieved naturally by updating the positional encoding in Transformers with input-dependent matrices. We developed two variants of *MapFormers* that unify absolute and relative positional encoding to model episodic (EM) and working memory (WM), respectively. We tested *MapFormers* on several tasks, including a classic 2D navigation task, showing that our models can learn a cognitive map of the underlying space and generalize OOD (e.g., to longer sequences) with near-perfect performance, unlike current architectures. Together, these results demonstrate the superiority of models designed to learn a cognitive map, and the importance of introducing a structural bias for structure-content disentanglement, which can be achieved in Transformers with input-dependent positional encoding. *MapFormers* have broad applications in both neuroscience and AI, by explaining the neural mechanisms giving rise to cognitive maps, while allowing these relation models to be learned at scale.

<sup>1</sup>Institut Jean Nicod <sup>2</sup>Laboratoire de Sciences Cognitives et Psycholinguistique (LSCP) <sup>3</sup>Département d'Études Cognitives, ENS, EHESS, CNRS, PSL University, Paris, France. Correspondence to: Victor Rambaud <victor.rambaud@gmail.com>, Salvador Mascarenhas <salvador.mascarenhas@ens.fr>, Yair Lakretz <yair.lakretz@gmail.com>.

Preprint. February 9, 2026.

## 1. Introduction

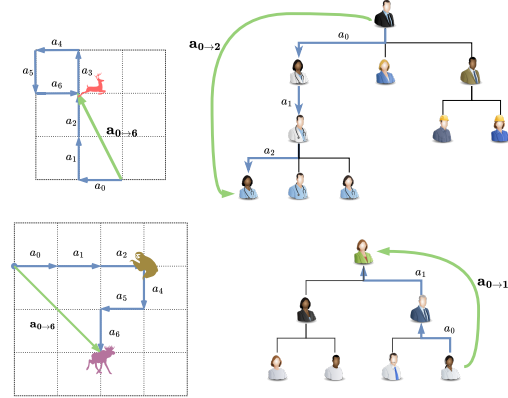


**Figure 1. Cognitive Maps and Path Integration: Factorizing Structure and Content.** Cognitive maps factorize entities from their position (or “state”) within a relational structure. Actions (blue arrows) update a position on the map—such as “step right” on a grid or “manager of” in an organization chart—and have a consistent, position-invariant effect across all environments. *Path integration* can be achieved by sequentially combining actions together  $a_{0 \rightarrow t} = (a_{t-1} \circ \dots \circ a_0)$  (green arrow).

Transformer-based models have revolutionized AI, sparking debate over whether we are on the verge of achieving Artificial General Intelligence (Bubeck et al., 2023; Morris et al., 2024). Yet, beneath their impressive performance, these models remain surprisingly brittle; when carefully tested, they often fail to generalize to out-of-distribution tasks that humans and animals can handle with ease (Nezhurina et al., 2024; Zhang et al., 2024). This gap suggests that Transformers might still lack the necessary structural biases that allow biological brains to navigate unknown scenarios and reason through novel problems efficiently.

A potential explanation for this gap lies in the ability to construct *cognitive maps* (Behrens et al., 2018): internal models of the world that capture the relationships among entities or events in the world. Cognitive maps separate the abstract, invariant *structure* of an environment from its specific, variable *content*. By disentangling the “where” from the “what”, biological systems can apply a known structure to entirely new observations. Structure-content separation is important for both spatial navigation (e.g., finding a shortcut

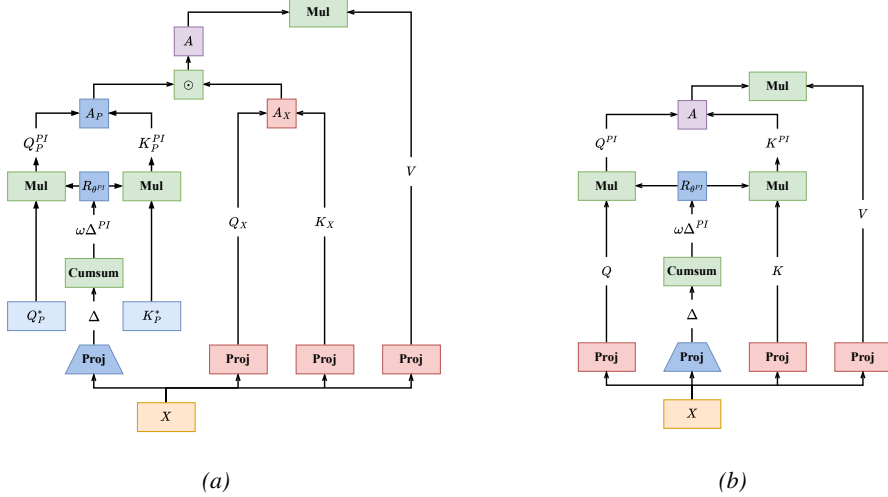


Figure 2. Disentangling Structure and Content for Path Integration in Episodic and Working Memory Transformers. Overview of our *MapFormers* architectures inspired by models of Episodic (EM; panel a) and Working Memory (WM; panel b) from (Whittington et al., 2025). In both cases, rotation angle  $\theta = \omega\Delta$  is obtained via a low-rank projection of input  $X$ , before computing a cumulative sum (cumsum) along the temporal dimension, to perform path integration (PI) in parallel:  $\theta^{PI} = \omega\Delta^{PI} = \omega \cdot \text{cumsum}_t(\Delta)$ . Input-dependent, block-diagonal, rotation matrices  $R_{\theta^{PI}}$  represent path-integration in the learned cognitive map. (a) **Episodic Memory MapFormer (MapEM)** with two parallel attentions  $A_X$  and  $A_P$ . The former captures raw similarities between external inputs and the latter encodes the problem’s structure. In *MapEM*, absolute position embeddings is obtained via path integration of initial position  $P^*$ , which can be initialized separately for keys and queries  $Q_P^*$  and  $K_P^*$ . (b) **Working Memory MapFormer (MapWM)** with relative positional encoding, where  $Q$ ,  $K$  are rotated via input-dependent matrix  $R_{\theta^{PI}}$ . In *MapWM*,  $\theta$  is learned, but keeping it fixed gives exactly RoPE. Diagrams created with Draw.io.

to get back home or finding a detour around an obstacle) and non-spatial, conceptual information (e.g., inferring family relations). Seeing structure as a connected graph of relations unifies such different domains: nodes represent states, while edges represent the relationships between them, spatial or conceptual. In a world where possible observations are unbounded but the underlying structure remains fixed, this factorization of structure and content provides the basis for flexible intelligence that modern AI has yet to master.

To navigate a structure, an agent must learn the set of *actions* that affect its state and, crucially, how these actions combine. This is called *path integration* (fig. 1, green arrows) – the process of integrating a sequence of actions, which is essential for tracking state changes and for mental planning (Ólafsdóttir et al., 2018). For example, knowing how the four cardinal directions (North, South, East, West) interact is sufficient to define any novel trajectory on a grid. Path integration can also enable an agent to plan shortcuts or bypass obstacles by recognizing that distinct action sequences, such as  $(\uparrow, \rightarrow, \rightarrow, \downarrow)$  and  $(\rightarrow, \rightarrow)$ , are functionally equivalent. Similarly, in a conceptual map, one can identify “Bob” as Alice’s uncle when told “Bob is the brother of Alice’s mother” by mentally composing these individual social relations into a direct relational link. Humans and animals are highly proficient at this type of relational composition (Hafting et al., 2005; Howard et al., 2014; Wehner & Srinivasan,

1981), a capability for robust out-of-distribution generalization that current AI systems still struggle to replicate (Vafa et al., 2024; Kaesberg et al., 2025).

What kind of structural bias must be introduced into a neural architecture to enable it to effectively learn a cognitive map and perform robust path integration? Previous work made progress in modeling cognitive maps using RNNs with *action-dependent* matrices (Whittington et al., 2019; 2025), allowing them to solve structure-dependent tasks and generalize to unseen scenarios. Although very promising, these models do not scale since (1) their action-dependent matrices need to be sequentially multiplied to perform path integration, making them slow to train and incompatible with parallel sequence processing, and (2) the models can only be applied to problems where the underlying structure is already known (for example, where the number of actions is known rather than learned).

To address this, we introduce *MapFormers*, a class of transformers that learn context-dependent cognitive maps with a generic neural mechanism, allowing the learning of structure at larger scale. *MapFormers* compute path integration *in parallel* and therefore allow scaling up to complex problems. Furthermore, *MapFormers* are trained in a fully self-supervised manner, and learn by themselves to disambiguate between actions and observations, which have opposite effects on the learned representations. Actions update the

internal state’s structure via learned operations but leave its semantic content untouched, while observations leave the internal structure fixed but change the state’s content. Empirically, we argue that *MapFormers*, to the best of our knowledge, are the first generic architectures to learn cognitive maps and generalize to longer sequences without supervision, and with minimal assumptions about the underlying structure. We introduce two variants of *MapFormers*, which unify relative rotary (RoPE; Su et al. 2023) and absolute positional embeddings, respectively as models of working and episodic memory, confirming the fundamental role that action-dependent positional embeddings play in encoding the location of tokens within a context-dependent cognitive map (Whittington et al., 2022). Finally, we draw theoretical arguments from Lie-group theory to characterize the class of structures that sequence-processing models are able to learn, allowing us to show, for example, that diagonal matrices used in current selective State Space Models are not expressive enough to learn cognitive maps.

## 2. Related Literature

In seminal work, Whittington et al. (2019) presented a set of tasks, for both spatial (navigation) and non-spatial (e.g., family trees) problems, which require learning a cognitive map in order to achieve strong generalization abilities. The Tolman-Eichenbaum Machine (TEM) was suggested as a model of the entorhinal and hippocampus regions, which can learn cognitive maps to solve these tasks. Specifically, TEM is an RNN-based architecture that uses *action-dependent* weights to update its position, before querying a Hopfield memory module (Ramsauer et al., 2021) with its updated position to retrieve what was seen at a previously visited location.

Whittington et al. (2025) extended the framework to model the role of the prefrontal cortex (PFC) in working memory, representing structure *implicitly*, by rotating the full neural activity into structured activity slots with action-dependent matrices. Whittington et al. (2022) show that TEM can be seen as a Transformer (TEM-t), where positional embeddings represent abstract positions in a *cognitive map*. However, TEM-t cannot leverage the parallel sequence processing abilities of Transformers since it requires the sequential updates of positional embeddings with action-dependent matrices, showcasing a core limitation of *actionable* models.

In line with TEM-t, other work has demonstrated the generalization power of sequence-dependent positional encoding in transformers (Golovneva et al., 2024; Zhu et al., 2025; Gopalakrishnan et al., 2025), yielding superior results in length generalization and a selection of formal tasks, but their representation power is poorly understood. Specifically, little is known about what kind of structural features these models can or cannot learn. Moreover, no connections

have been made to cognitive maps and path integration, which is one of the main goals of *MapFormers*.

## 3. General Setup

### 3.1. Tasks

To study the performance and OOD generalization of *MapFormers*, compared to baseline models, we focused on two main tasks:

**Selective Copy** This task was introduced in Mamba (Gu & Dao, 2024) and used in CoPE (Golovneva et al., 2024) to study whether the model is able to ignore distractors, which transformers with static positional encoding like RoPE (Su et al., 2023) are unable to do. The model receives a sequence of symbols and needs to copy it fully while ignoring a blank token  $B : CFEABBCBF \rightarrow CFEACF$ . Solving this task requires a flexible gating mechanism that baseline transformers do not possess.

**Forced-Navigation Task** Following the task proposed by Whittington et al. (2019), we formulate the learning problem within a standard self-supervised setup. This task consists of a random sequence of symbols  $s = (a_1, o_1, \dots, a_T, o_T)$  with action  $a_t$  sampled from  $\{\uparrow, \downarrow, \rightarrow, \leftarrow\}$  and observation  $o_t$  from  $\{o_1, \dots, o_K\}$ , a finite set of  $K$  objects, plus a blank token  $B$  when the location is empty. The model is asked to predict the upcoming observation each time it comes back to a previously visited location. To solve the task and generalize OOD, the model needs to represent the underlying 2D grid structure of the problem, independently of the specific observations (content) that appear randomly in the training data. The model also needs to understand that only action tokens update position, and distinguish them from observation tokens.

### 3.2. Cognitive Maps and Additive Path-Integration

We define a cognitive map as a discrete multirelational graph  $G = (N, E, \mathcal{R}, L)$ , where nodes  $N$  represent states and  $E$  is the set of edges. The set  $\mathcal{R} = \{r_1, \dots, r_m\}$  denotes a finite set of cardinal relations, and  $L : E \rightarrow \mathcal{R}$  is a labeling function that assigns each edge to a specific relation type. An agent navigating this map occupies a position  $p \in N$  and possesses a set of cardinal actions  $\mathcal{A} = \{a_1, \dots, a_m\}$ . Each action  $a_i$  is defined as a mapping  $a : N \rightarrow N$ , such that applying an action  $a_t \in \mathcal{A}$  at a position  $p_t$  at time  $t$  results in a new position  $p_{t+1} = a_t(p_t) \in N$ .

In order to successfully navigate the map, the agent needs to learn the actions in  $\mathcal{A}$  such that they align with the structural relations in  $R$ . Specifically, for any relation  $r_{j \rightarrow i} \in R$  connecting  $n_j$  to  $n_i$ , the agent needs to learn an action  $a_t \in \mathcal{A}$  that satisfies the condition  $p_{t+1} = a_t(p_t = n_j) = n_i$ . This alignment ensures that the agent’s internal operators accu-

rately reflect the graph’s topology, allowing for predictable transitions through the state space.

Given  $\mathcal{A}$ , the agent can perform *path integration* (fig. 1, green arrows) by composing a sequence of actions. The resulting position  $p_i$  reached from an initial position  $p_j$  through a sequence of actions is defined by:

$$p_i = a_{j \rightarrow i} p_j = (a_{i-1} \circ \dots \circ a_j) p_j$$

Where we denoted integrated actions as  $a_{j \rightarrow i} = a_{i-1} \circ \dots \circ a_j$ . Note that position is always defined by integrated action  $a_{j \rightarrow i}$ , representing either relative or, when referenced to the origin  $p_0$  ( $j = 0$ ), absolute position.

In previous work, Whittington et al. (2019; 2022; 2025) modeled cognitive maps in RNNs with *action-dependent* recurrent weights, to compute integrated actions  $a_{j \rightarrow i}$  via matrix multiplication:  $\mathbf{W}_{j \rightarrow i} := \prod_{s=j}^{i-1} W_{a_s}$ . These matrices are required to form a Lie group, in order to have properties such as closure, an identity (null action) and inverse element, which allows—for compact groups—to represent  $W_a$ ’s as block-diagonal matrices (Dorrell et al., 2023).

We pursue this line of work but avoid sequential matrix multiplications  $\prod_{s=j}^{i-1} W_{a_s}$ , which are computationally demanding, and instead compose actions *linearly*, allowing efficient path integration. To achieve this, we compute path integration in the Lie algebra and map the result onto the Lie group using the exponential map (sec. A.1).

For example, in the case of 2D rotations, action-dependent matrices are rotation matrices  $R_\theta$  that lie on the manifold of the special orthogonal group  $\text{SO}(2)$ . Its Lie algebra  $\mathfrak{so}(2)$  is one-dimensional, possessing a single generator matrix  $S$  (the unit skew-symmetric matrix;  $S^T = -S$ ), which spans the vector space of the algebra. Any matrix in  $\mathfrak{so}(2)$  can be expressed as  $A = \omega S$ , where  $\omega$  is the angular velocity. A finite rotation  $R_\theta$  can then be generated by integrating the infinitesimal angular velocities  $\omega$  over a duration  $\Delta_t$ . Mapformers can compute path integration at the level of the Lie algebra by summing the integration durations  $\Delta_t$ ’s:

$$W_{j \rightarrow i} := \exp \left( \omega S \sum_{t=j}^{i-1} \Delta_t \right) := R(\theta_{j \rightarrow i}), \quad (1)$$

Most of the computational cost thus boils down to a simple sum  $\sum_{t=j}^{i-1} \Delta_t$ . Computing the exponential map needs to be done only once, after the summation; furthermore, in the case of rotation, it is not strictly necessary, as the closed-form solution for the exponential map is already known to be the standard rotation matrix  $R_\theta$  (sec. A.2,3,6&7).

In practice, in the case of navigation on a finite 2D grid, *i.e.* a torus, action-dependent matrices are  $2 \times 2$  block-diagonal rotations in  $\text{SO}(2)$ , where each block is defined by

a constant *angular velocity*  $\omega_b$ . They represent rotations at different scales, and are learned by the model during training, adapting themselves to the size of the grid – e.g., larger grids require a smaller  $\omega$  to avoid wrapping around. Path integration can be computed along each of the  $n_b$  blocks, in parallel.

Interestingly, the exponential map also appears following the *discretization* step of continuous State Space Models (SSMs) (Gu & Dao, 2024), by a step size  $\Delta$ . The continuous and discrete version of the SSM equations can thus be seen as describing dynamics occurring in a 1-dimensional Lie algebra and Lie group, respectively. Since Linear Transformers are equivalent to SSM (Dao & Gu, 2024), in this work, we mainly focus on  $\text{SO}(2)$ , as it’s the only 1-dimensional compact Lie-group. Compactness is desired since a finite neural population can only represent a bounded cognitive map. This ensures commutativity, hence linear path-integration, and a closed-form solution of the exponential map (see sec. B.2 for non-abelian groups).

## 4. Models

In this section, we introduce two new Transformer-based architectures, which we call **MapFormers**, designed to learn path integration and, consequently, cognitive maps. The fundamental mechanism in both *MapFormers* is the use of *input-dependent matrices* to update positional encoding as in sec. 3.2, which, as explained, represents position in a *context-dependent* cognitive map instead of ordinal order used in standard Transformers.

Transformers achieve parallel and large-scale sequence processing via the attention mechanism. An input sequence  $X \in \mathbb{R}^{l \times d}$  is projected into keys, queries and values,  $Q, K, V \in \mathbb{R}^{l \times d}$ , and token mixing is achieved via a weighted sum of the values based on the key-query similarity matrix  $A \in \mathbb{R}^{l \times l}$ :

$$\mathbf{Att}(Q, K, V) = \text{softmax} \left( \frac{QK^T}{\sqrt{d}} \right) V$$

Since the attention mechanism is permutation-invariant, positional information must be provided, either through absolute positional embeddings added to the input (Vaswani et al., 2017), or relative positional encoding to model the distance between keys and queries (Su et al., 2023).

The two proposed architectures (fig. 2a & 2b) follow this distinction: the first architecture extracts and represents structural information *separately* from the content, using absolute positional embeddings to form a cognitive map; this is akin to a model of episodic memory (Whittington et al., 2019). The second architecture, conversely, represents structure *implicitly* by rotating neural activity into distinct subspaces, akin to the models of working memory in Whittington et al. (2025).

To learn a cognitive map, the model has to identify that action tokens ( $s_t = a_t$ ) update the internal position  $p_t$ , while ensuring that observations ( $s_t = o_t$ ) leave the structure untouched. To optimize this process, the model learns the rotation duration rather than the matrix itself, as in eq. 1. Specifically, the model maps a token representation  $x_t \in \mathbb{R}^d$  to a per-block *integration duration*  $\{\Delta_{t_b}\}_b = f_\Delta(x_t) \in \mathbb{R}^{n_b}$ , and builds from it the final rotation angles  $\theta_t = \{\omega_b \Delta_{t_b}\}_b$ .

Then, rotations are aggregated in parallel along the temporal dimension  $\theta_{0 \rightarrow t} := \text{cumsum}_t(\theta_t)$  to build the final block-diagonal, integrated rotation matrix  $R_{\theta_{PI}} := \{R_{\theta_{0 \rightarrow t}}\}_{t \leq l} \in \mathbb{R}^{l \times d \times d}$  (fig. 2a & 2b). Here,  $\omega \in \mathbb{R}^{n_b}$  represents the *angular velocities* on each rotation block, a parameter learned by the model during training (see sec. A.7 & A.8 for more details).

#### 4.1. MapFormers: Path-Integrating Transformers for learning Cognitive Maps

**MapEM: MapFormers with Absolute Positional Embeddings as Models of Episodic Memory (EM)** The first architecture of *MapFormers* makes use of absolute positional embeddings to learn a cognitive map (fig. 2a), inspired by the links established between TEM and transformers – TEM-t (Whittington et al., 2022). Once  $R_{\theta_{PI}}$  is computed, one only needs to learn an embedding  $p_0 \in \mathbb{R}^d$ , representing the *origin* of the cognitive map, such that:

$$P := R_{\theta_{PI}} P^*; \quad P^* = [p_0, \dots, p_0]_l \in \mathbb{R}^{l \times d}$$

Attention is computed on  $Q_G := \{q_t^g = \text{vec}(q_t^\top \cdot p_t)\}_{t \leq l} \in \mathbb{R}^{l \times d^2}$  and  $K_G$ , the conjunctions of **what** has been seen and **where** (fig.2a). This can be reframed as the element-wise product of content and position attentions  $A_X = Q_X K_X^\top / \sqrt{d}$  and  $A_P = P \cdot P^\top / \sqrt{d}$ , computed separately (still in parallel by concatenating the heads, see sec. A.7), such that  $A_P$  acts as an attention mask on  $A_X$ :

$$\text{Att}(Q_g, K_g, V) = \text{softmax}(A_X \odot A_P) V \quad (2)$$

This allows modeling Episodic Memory in a transformer that we call *MapFormer-EM* (or *MapEM*, in short, see sec. A.4 for details on EM models).

**MapWM: MapFormers with Relative Positional Embeddings as a Model of Working Memory** In (Whittington et al., 2025), Working Memory RNNs represent structure *implicitly* by shifting neural activity into structured activity slots with action-dependent matrices. This directly models the logic of RoPE (Su et al., 2023), where a fixed rotation matrix modeling relative distance is directly applied on the keys and queries, *i.e.* the state. In *MapFormers-WM* (*MapWM*; 2b)), keys and queries are rotated by  $R_{\theta_{PI}}$ , which encodes their relative distance in the cognitive map. We further formalize the links between *MapWM* and models of working memory in sec. A.6.

#### 4.2. Baseline models

In all experiments, we compare *MapFormers* to a classic Transformer architecture with static positional encoding, as well as two architectures learning input-dependent positional encoding serving as baselines for structure learning models.

**Rotary Position Embedding (RoPE)** (Su et al., 2023) is used as our baseline Transformer since it is the most popular (fixed) position encoding architecture, and is analogous to our *MapWM* model without input selectivity, theoretically incapable of learning input-dependent matrices and structure-based problems.

**Contextualized Positional Encoding (CoPE)** (Golovneva et al., 2024) compresses relative distances with a cumulative gating mechanism, reminding path integration. Since the sigmoid gate can only take positive values, the model cannot represent an action and its inverse. Moreover, since CoPE only compresses relative ordinal distance, it should not be able to represent structure in higher dimensions.

**Contextualized Equivariant Position Embedding (TAPE)** (Zhu et al., 2025) learns to modify its positional encoding after the attention mechanism, with input-dependent MLPs. However, TAPE exhibits several issues: First, updating structure after the attention means that the learned structure depends on the *previous* and not the *current* layer. Second, TAPE’s positional embedding are updated based on the attention scores and not path integration, giving no theoretical guaranty to integrate structure over long ranges.

**MapEM-s and MapEM-o** can choose to balance between observation  $o$  and structure  $s$ , giving rise to *MapEM-s*, *MapEM-o* or *MapEM-os* by choosing to use either structure, observation or both in eq. 2, respectively.

## 5. Results

### 5.1. MapFormers Solve the Selective-Copy Task

We start by evaluating *MapFormers* on the selective-copy task defined in sec. 3.1, compared to baseline models, following the training setup of (Golovneva et al., 2024). Since CoPE is able to solve this task by compressing token positions, we hypothesize that *MapFormers* will achieve similar results by encoding position on a 1D circle, using learned rotation. TAPE does not have theoretical guaranties for performing path integration, so we anticipated it would fail on OOD generalization. Tab. 5 shows that, indeed, only *MapFormers* and CoPE generalize OOD. Interestingly, TAPE improves performances in shorter sequences over RoPE, by learning a form of position interpolation, but performances deteriorate on longer sequences. In sum, these results show the importance of path integration for solving the selective-copy task.

	IID	OOD Dense	OOD Sparse
MapEM-o	0.11	0.08	0.07
MapEM-s	0.10	0.11	0.10
RoPE	<b>1.0</b>	0.48	0.22
TAPE	<b>1.0</b>	0.88	0.10
CoPE	<b>1.0</b>	<b>1.0</b>	<b>1.0</b>
<b>MapWM</b>	<b>1.0</b>	<b>1.0</b>	<b>1.0</b>
<b>MapEM-os</b>	<b>1.0</b>	<b>1.0</b>	<b>1.0</b>

Table 1. **Selective copy accuracy.** IID sequences have 128/128 blank/non-blank tokens. OOD: dense 64/128, sparse 256/128. RoPE solves the task IID but fails to generalize OOD, TAPE improves generalization on shorter sequences but not on long sequences. As expected, both CoPE and MapFormer can solve it, showing that the latter can also learn gating mechanisms. MapEM-o and MapEM-s cannot solve this task, since it requires both "sensory" inputs (the tokens to copy) and structure (the tokens to ignore).

## 5.2. MapFormers Solve the Grid Navigation Tasks but not Baseline Models

We next evaluated MapFormers on the navigation tasks in 1D and 2D (sec. 3.1). Because observations are random, to solve this task and generalize OOD a model needs to build coherent representations of actions and aggregate them sequentially. We therefore hypothesized that only MapFormers would achieve strong OOD generalization on these tasks given their ability to perform both path integration and motion on a torus, approximating a 2D plane. Since CoPE uses gating and cannot represent an action and its inverse, we expect it to fail even in 1D. Tab. 2 confirms that 1-layer MapFormers solve the task and generalize OOD, unlike baseline models, even with up to 4 layers. These results highlight the benefits of having a structural bias for path integration, and thus the ability to create a cognitive map of the external environment.

## 5.3. MapEMs are more Computationally Demanding but scale better than MapWMs

Compared to MapFormer-WM, MapFormer-EM queries its memories with the conjunction of observational and structural features, which requires a second pool of neurons  $p_t \in \mathbb{R}^d$  as well as computing two attention matrices  $A_X$  and  $A_P$  separately. This offers sparser and higher dimensional features  $g_t = \text{vec}(x_t, p_t^\top) \in \mathbb{R}^{d^2}$  (fig. 5a) but doubles the computational load of the attention operation, which is already the main bottleneck in scaling transformers.

This factorization in two separate pools of neurons should allow EM to be more efficient than WM, as in the former, neurons specialize for either position or observation. To test this, we conducted three experiments to understand the effect of sequence length, model size and vocabulary size on performance, by varying each time one parameter while

	1D navigation			2D Navigation		
	IID	OOD		IID	OOD	
		D	S		D	S
MapEM-o	0.14	0.20	0.12	0.16	0.08	0.08
RoPE (1L)	0.24	0.39	0.16	0.33	0.35	0.29
RoPE (2L)	0.28	0.42	0.15	0.33	0.31	0.29
RoPE (4L)	0.20	0.31	0.11	0.33	0.32	0.28
TAPE (1L)	0.23	0.40	0.15	0.32	0.32	0.25
TAPE (2L)	0.52	0.44	0.22	0.59	0.38	0.27
TAPE (4L)	0.54	0.43	0.24	0.58	0.36	0.28
CoPE (1L)	0.58	0.74	0.42	0.66	0.74	0.59
CoPE (2L)	0.67	0.74	0.57	0.63	0.72	0.52
CoPE (4L)	0.72	0.83	0.62	0.67	0.73	0.57
<b>MapWM</b>	<b>1.0</b>	<b>1.0</b>	<b>1.0</b>	<b>0.99</b>	<b>0.99</b>	0.96
<b>MapEM-os</b>	<b>1.0</b>	<b>1.0</b>	<b>1.0</b>	<b>1.0</b>	<b>0.99</b>	0.97
<b>MapEM-s</b>	<b>1.0</b>	<b>1.0</b>	<b>1.0</b>	<b>1.0</b>	<b>1.0</b>	<b>0.99</b>

Table 2. **1D-2D grid navigation accuracy.** IID sequences have 128/64 sequence length/grid width. OOD: dense (D) 64/32, sparse (S) 256/128. Neither RoPE and TAPE solve the task. CoPE performs better but also fails, even in 1D, since it cannot learn the inverse of an action (forward/backward). Even with additional layers compared to Mapformers, all baseline models fails. In contrast, MapFormers solved the task and perfectly generalized OOD, even if performances slightly degrade in 2D on longer sequences (OOD-s). This is since the amount of coordinates to represent increases quadratically with length. As expected, the control model MapEM-o performs even worse than RoPE, since it does not encode position.

keeping the others fixed. Fig. 3 shows that, indeed, EM models scale better than WM, consistently with previous results (Whittington et al., 2025). Also, MapEM-s (blue curves), which relies on position alone, is more robust to both sequence length (fig. 3a) and model size (fig. 3b), since sensory features only add noise in this task. Last, having a sufficiently large number of neurons is crucial for both learning a cognitive map (fig. 3a, models fail to converge with  $h = 16$ ) and memorizing large sets of objects (fig. 3c). In sum, these results demonstrate the superior capacity of MapEM models in recall tasks, at the cost of doubling the attention computation.

## 5.4. Interpretability Analysis: Observations are Vectors, Actions are Matrices

In the tasks, some symbols (actions  $s_t \in \{\uparrow, \downarrow, \rightarrow, \leftarrow\}$ ) must update the model's position on its cognitive map, while others should leave position the same (observations) and instead modify its content. The model must learn by itself which ones are actions and which ones are observations. How can we tell whether MapFormers have learned this and therefore have learned a cognitive map?

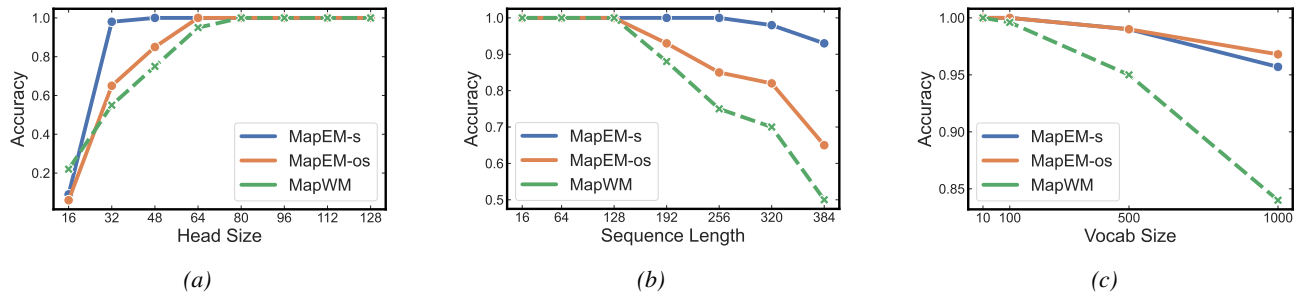


Figure 3. **Behavioral Analyses: MapEM scales better than MapWM.** Comparison of *MapEM*-s, *MapEM*-os, and *MapWM* robustness across model size, sequence length, and vocabulary size. **(a)** Train accuracy vs. head size (fixed sequence length  $l = 256$ , vocabulary size  $v = 16$ ). *MapEM* requires fewer units than *MapWM* to achieve high performance. **(b)** Train accuracy vs. sequence length (fixed head size  $h = 48$ , vocabulary  $v = 16$ ). EM models exhibit greater robustness to increasing sequence lengths. **(c)** Train accuracy vs. vocabulary size (fixed head size  $h = 32$ , sequence length  $l = 16$ ). EM models outperform WM models in retaining an increasing number of items.

For this, we first compared the learned integration durations  $\Delta_t$ , since they define how the cognitive map is updated. Fig. 4a compares model performance and integration durations during training. It shows that perfect generalization is achieved as soon as the model learns that action tokens  $a_t$  trigger state rotations while observation tokens  $o_t$  leave it untouched. Next, we studied the representation of action tokens, after training. Tab. 4b-top & fig. 4d show that opposite actions (left / right or up / down) cancel each other, pointing to opposite direction, and representations of observations are all projected to zero. That is, only action tokens  $a_t$  can update the cognitive map. Conversely, only observations need to update the state’s content, since  $\|v_{o_t}\| \gg \|v_{a_t}\|$ , as fig. 4d-bottom & fig. 4f confirm.

From a point of view of Lie-group theory, actions are represented within the space of the Lie algebra  $\mathfrak{g}$ , whereas observations  $v_t$  belong to the content space, the traditional latent space of transformers. Therefore, in *MapFormers*, actions are matrices and observations are vectors, which is reminiscent of ideas presented by Baroni & Zamparelli (2010), where nouns are vectors and adjectives are matrices, giving the model stronger OOD generalization compared to baseline models.

## 6. Discussion

We introduced *MapFormers*, a novel class of Transformer-based architectures designed to learn cognitive maps and perform parallel path integration in a self-supervised setup. *MapFormers* address the key limitations of previous RNN-based models in order to scale to complex, long-sequence problems: (1) they leverage the parallel processing ability of Transformers; (2) they offer greater flexibility by reducing the need to assume the underlying structure and learn when to update or not the cognitive map. We developed two variants, *MapFormer*-WM (Working Memory) and *MapFormer*-EM (Episodic Memory), which unify relative and absolute positional embeddings, respectively, as

computational models of these distinct memory systems. Critically, we provide theoretical arguments from Lie-group theory—extending the theoretical framework of actionable representations (Dorrell et al., 2023)—to understand the class of structures that will be represented within a *MapFormer*’s positional encoding (sec. A.1 & B.2).

*MapFormers* achieved near-perfect OOD generalization on longer, sparser sequences, significantly outperforming baselines. While CoPE matched *MapFormers* on simple gating tasks – consistent with theoretical expectation – TAPE failed to generalize across all tasks since this type of model does not explicitly path integrate (sec. 5.1). Crucially, on complex tasks that require forming a cognitive map, only *MapFormers* succeeded (sec.5.2). This shows that updating positional encoding with input-dependent matrices—endowed with the appropriate group structure—is essential for true structural generalization rather than reliance on heuristics. Finally, probing the internal representations of the model, we found consistent evidence that *MapFormers* have indeed learned to represent a cognitive map.

While we mainly explored rotation matrices for computational efficiency, more complex group structures can be learned by *MapFormers*. This allows notably to explore structures where the irreducible representations (*irreps*, Dorrell et al. 2023, sec. A.1) are unknown, like rotations in high dimensions or non-commutative groups. This might affect inference speed; that is, a tradeoff between expressibility and processing time needs to be found (sec. B.2).

In summary, *MapFormers* (1) address the issues of previous actionable models (Whittington et al., 2019; 2022; 2025) by enabling the learning of cognitive maps at scale; (2) unify absolute and relative positional encoding with models of Episodic Memory (EM) and Working Memory (WM); (3) give a comprehensive view of how to learn structure in Transformers, unlike previous attempts (Zhu et al., 2025; Golovneva et al., 2024; Gopalakrishnan et al., 2025); (4) empirically demonstrate that *MapFormers* are the only cur-

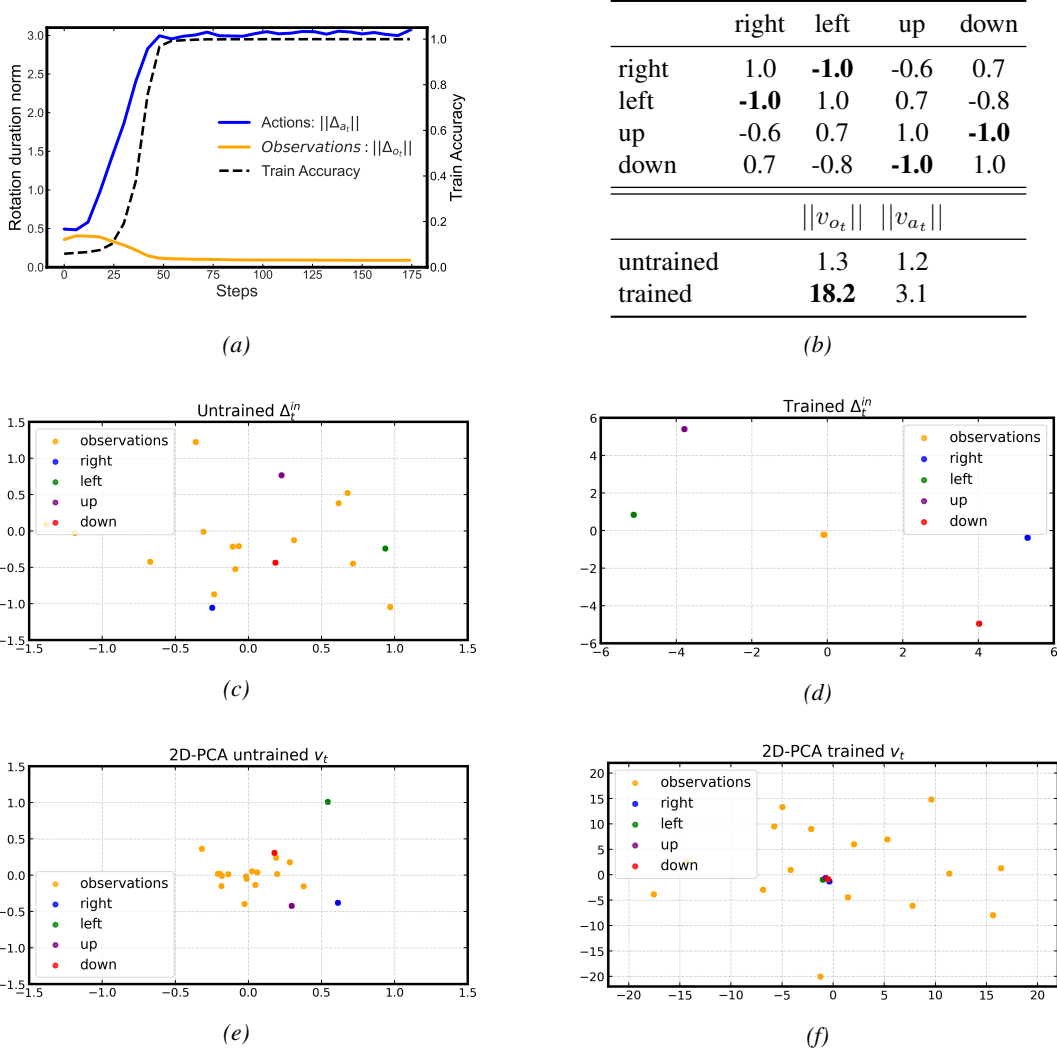


Figure 4. **Neural Analyses: Actions are Matrices and Observations are Vectors.** (a) Norm of rotation duration  $\|\Delta_t\|$  vs Accuracy through training. *MapFormers* reaches perfect accuracy as soon as it learns that action tokens  $a_t$  (blue curve) update the agent’s position while observation tokens  $o_t$  (orange curve) leave it untouched via 0-angle rotations, *i.e.*  $R_{\theta_o} \approx I_n$  (b) (top table) Action’s movement in the Lie algebra  $\Delta_{a_t}^{in}$  cosine similarities. Opposite actions (right v left / up v down) cancel each other ( $\cos(\Delta_{left}^{in}, \Delta_{right}^{in}) = -1$ , but orthogonal dimensions are not projected onto orthogonal axes ( $|\cos(\Delta_{left}^{in}, \Delta_{up}^{in})| \gg 0$ ). Other constraints, such as bounded energy (Whittington et al., 2023), could be added to force disentanglement (bottom table). Once trained, the norm of value embeddings  $v_t$  in the attention layer becomes much bigger for observations than actions ( $\|v_{o_t}\| \gg \|v_{a_t}\|$ ), implying that only observations contribute in updating the state’s content. (c) An untrained *Mapformer* projects observations and actions randomly (d) After training, observation tokens are all projected towards 0 (orange), while tokens representing opposite directions (left / right or up / down) are all projected to opposite directions. (e) An untrained *Mapformer* projects values  $v_t$  randomly. (f) After training, action tokens are projected towards zero.

rent transformer-based architecture to perfectly generalize OOD on structure-dependent tasks.

### 7. Limitations

We highlight several limitations of our work that we leave for future explorations. First, in order to compute *path integration*, we sum the rotation angles along the temporal dimension, meaning that our formalism only applies to causal transformers. Further work is needed to generalize

our method to non-causal problems such as visual processing, but the same methods used to adapt SSMs to vision (Zhu et al., 2024) could be used. Second, we did not try to scale our method to larger model sizes and larger datasets, but since *MapFormers* require little extra compute compared to baseline transformers, processing speed should not be a bottleneck. Finally, our results only confirm the superiority of EM models on recall tasks compared to their WM counterparts, but further experiments should compare these two models on more complex tasks such as reasoning.

## Impact Statement

The scalability and structural flexibility of *MapFormers* suggest they could serve as generic architectures for a variety of complex tasks beyond spatial navigation, including language modeling, vision, and protein folding (Siméoni et al., 2025; Jumper et al., 2021). By framing the learning of cognitive maps through a Lie-group theoretic lens, our work provides a path toward disentangling abstract structures from raw content. Furthermore, while this work focused on rotation matrices for efficiency, the ability of *MapFormers* to learn more complex group structures opens new doors for AI. It allows for the exploration of structures where irreducible representations are unknown, such as rotations in high-dimensional spaces or non-commutative groups. This offers a theoretical framework for understanding how biological and artificial agents might represent complex relational data, potentially leading to more robust, structure-aware AI systems that mirror the efficiency of human cognition.

## 8. Acknowledgments

This work has benefited from public funding from the IA-Cluster PR[AI]RIE-PSAI project, managed by the French National Research Agency (ANR) as part of the France 2030 program, reference “ANR-23-IACL-0008”. Ecole Normale Supérieure-PSL’s Département d’Etudes Cognitives is supported by ANR grants, ANR-10-IDEX-0001-02 and FrontCog, ANR-17-EURE0017.

## References

Baroni, M. and Zamparelli, R. Nouns are vectors, adjectives are matrices: Representing adjective-noun constructions in semantic space. In Li, H. and Márquez, L. (eds.), *Proceedings of the 2010 Conference on Empirical Methods in Natural Language Processing*, pp. 1183–1193, Cambridge, MA, October 2010. Association for Computational Linguistics. URL <https://aclanthology.org/D10-1115/>.

Behrens, T. E., Muller, T. H., Whittington, J. C., Mark, S., Baram, A. B., Stachenfeld, K. L., and Kurth-Nelson, Z. What is a cognitive map? organizing knowledge for flexible behavior. *Neuron*, 100(2):490–509, 2018. ISSN 0896-6273. doi: <https://doi.org/10.1016/j.neuron.2018.10.002>. URL <https://www.sciencedirect.com/science/article/pii/S0896627318308560>.

Bubeck, S., Chandrasekaran, V., Eldan, R., Gehrke, J., Horvitz, E., Kamar, E., Lee, P., Lee, Y. T., Li, Y., Lundberg, S., Nori, H., Palangi, H., Ribeiro, M. T., and Zhang, Y. Sparks of artificial general intelligence: Early experiments with gpt-4, 2023. URL <https://arxiv.org/abs/2303.12712>.

Dao, T. and Gu, A. Transformers are ssms: Generalized models and efficient algorithms through structured state space duality, 2024. URL <https://arxiv.org/abs/2405.21060>.

Dorrell, W., Latham, P. E., Behrens, T. E. J., and Whittington, J. C. R. Actionable neural representations: Grid cells from minimal constraints, 2023. URL <https://arxiv.org/abs/2209.15563>.

Golovneva, O., Wang, T., Weston, J., and Sukhbaatar, S. Contextual position encoding: Learning to count what’s important, 2024. URL <https://arxiv.org/abs/2405.18719>.

Gopalakrishnan, A., Csordás, R., Schmidhuber, J., and Mozer, M. C. Decoupling the “what” and “where” with polar coordinate positional embeddings, 2025. URL <https://arxiv.org/abs/2509.10534>.

Gu, A. and Dao, T. Mamba: Linear-time sequence modeling with selective state spaces, 2024. URL <https://arxiv.org/abs/2312.00752>.

Gu, A., Goel, K., and Ré, C. Efficiently modeling long sequences with structured state spaces, 2022. URL <https://arxiv.org/abs/2111.00396>.

Hafting, T., Fyhn, M., Molden, S., Moser, M.-B., and Moser, E. I. Microstructure of a spatial map in the entorhinal cortex. *Nature*, 436(7052):801–806, Aug 2005. ISSN 1476-4687. doi: [10.1038/nature03721](https://doi.org/10.1038/nature03721). URL <https://doi.org/10.1038/nature03721>.

Howard, L., Javadi, A., Yu, Y., Mill, R., Morrison, L., Knight, R., Loftus, M., Staskute, L., and Spiers, H. The hippocampus and entorhinal cortex encode the path and euclidean distances to goals during navigation. *Current Biology*, 24(12):1331–1340, 2014. ISSN 0960-9822. doi: <https://doi.org/10.1016/j.cub.2014.05.001>. URL <https://www.sciencedirect.com/science/article/pii/S0960982214005260>.

Jumper, J., Evans, R., Pritzel, A., Green, T., Figurnov, M., Ronneberger, O., Tunyasuvunakool, K., Bates, R., Žídek, A., Potapenko, A., Bridgland, A., Meyer, C., Kohl, S. A. A., Ballard, A. J., Cowie, A., Romera-Paredes, B., Nikolov, S., Jain, R., Adler, J., Back, T., Petersen, S., Reiman, D., Clancy, E., Zielinski, M., Steinegger, M., Pacholska, M., Berghammer, T., Bodenstein, S., Silver, D., Vinyals, O., Senior, A. W., Kavukcuoglu, K., Kohli, P., and Hassabis, D. Highly accurate protein structure prediction with alphafold. *Nature*, 596(7873):583–589, Aug 2021. ISSN 1476-4687. doi: [10.1038/s41586-021-03819-2](https://doi.org/10.1038/s41586-021-03819-2). URL <https://doi.org/10.1038/s41586-021-03819-2>.

- Kaesberg, L. B., Wahle, J. P., Ruas, T., and Gipp, B. SPaRC: A spatial pathfinding reasoning challenge. In Christodoulopoulos, C., Chakraborty, T., Rose, C., and Peng, V. (eds.), *Proceedings of the 2025 Conference on Empirical Methods in Natural Language Processing*, pp. 10359–10390, Suzhou, China, November 2025. Association for Computational Linguistics. ISBN 979-8-89176-332-6. doi: 10.18653/v1/2025.emnlp-main.526. URL <https://aclanthology.org/2025.emnlp-main.526/>.
- Knapp, A. W. and Knapp, A. W. *Lie groups beyond an introduction*, volume 140. Springer, 1996.
- Loshchilov, I. and Hutter, F. Decoupled weight decay regularization, 2019. URL <https://arxiv.org/abs/1711.05101>.
- Morris, M. R., Sohl-dickstein, J., Fiedel, N., Warkentin, T., Dafoe, A., Faust, A., Farabet, C., and Legg, S. Levels of agi for operationalizing progress on the path to agi, 2024. URL <https://arxiv.org/abs/2311.02462>.
- Nezhurina, M., Cipolina-Kun, L., Cherti, M., and Jitsev, J. Alice in wonderland: Simple tasks reveal severe generalization and basic reasoning deficits in state-of-the-art large language models. In *NeurIPS 2024 Workshop on Scientific Methods for Understanding Deep Learning*, 2024. URL <https://openreview.net/forum?id=Mk17dzjYiW>.
- Ólafsdóttir, H. F., Bush, D., and Barry, C. The role of hippocampal replay in memory and planning. *Current Biology*, 28(1):R37–R50, Jan 2018. ISSN 0960-9822. doi: 10.1016/j.cub.2017.10.073. URL <https://doi.org/10.1016/j.cub.2017.10.073>.
- Ramsauer, H., Schödl, B., Lehner, J., Seidl, P., Widrich, M., Adler, T., Gruber, L., Holzleitner, M., Pavlović, M., Sandve, G. K., Greiff, V., Kreil, D., Kopp, M., Klambauer, G., Brandstetter, J., and Hochreiter, S. Hopfield networks is all you need, 2021. URL <https://arxiv.org/abs/2008.02217>.
- Siméoni, O., Vo, H. V., Seitzer, M., Baldassarre, F., Oquab, M., Jose, C., Khalidov, V., Szafraniec, M., Yi, S., Ramamonjisoa, M., Massa, F., Haziza, D., Wehrstedt, L., Wang, J., Darcet, T., Moutakanni, T., Sentana, L., Roberts, C., Vedaldi, A., Tolan, J., Brandt, J., Couprie, C., Mairal, J., Jégou, H., Labatut, P., and Bojanowski, P. Dinov3, 2025. URL <https://arxiv.org/abs/2508.10104>.
- Su, J., Lu, Y., Pan, S., Murtadha, A., Wen, B., and Liu, Y. Roformer: Enhanced transformer with rotary position embedding, 2023. URL <https://arxiv.org/abs/2104.09864>.
- Vafa, K., Chen, J. Y., Rambachan, A., Kleinberg, J., and Mullainathan, S. Evaluating the world model implicit in a generative model, 2024. URL <https://arxiv.org/abs/2406.03689>.
- Vaswani, A., Shazeer, N., Parmar, N., Uszkoreit, J., Jones, L., Gomez, A. N., Kaiser, L. u., and Polosukhin, I. Attention is all you need. In Guyon, I., Luxburg, U. V., Bengio, S., Wallach, H., Fergus, R., Vishwanathan, S., and Garnett, R. (eds.), *Advances in Neural Information Processing Systems*, volume 30. Curran Associates, Inc., 2017. URL [https://proceedings.neurips.cc/paper\\_files/paper/2017/file/3f5ee243547dee91fbd053c1c4a845aa-Paper.pdf](https://proceedings.neurips.cc/paper_files/paper/2017/file/3f5ee243547dee91fbd053c1c4a845aa-Paper.pdf).
- Wang, S., Li, B. Z., Khabsa, M., Fang, H., and Ma, H. Linformer: Self-attention with linear complexity, 2020. URL <https://arxiv.org/abs/2006.04768>.
- Wehner, R. and Srinivasan, M. V. Searching behaviour of desert ants, *genuscataglyphis* (formicidae, hymenoptera). *Journal of comparative physiology*, 142(3):315–338, Sep 1981. ISSN 1432-1351. doi: 10.1007/BF00605445. URL <https://doi.org/10.1007/BF00605445>.
- Whittington, J. C., Muller, T. H., Mark, S., Chen, G., Barry, C., Burgess, N., and Behrens, T. E. The tolmán-eichenbaum machine: Unifying space and relational memory through generalisation in the hippocampal formation. *bioRxiv*, 2019. doi: 10.1101/770495. URL <https://www.biorxiv.org/content/early/2019/09/24/770495>.
- Whittington, J. C., Warren, J., and Behrens, T. E. Relating transformers to models and neural representations of the hippocampal formation, 2022. URL <https://arxiv.org/abs/2112.04035>.
- Whittington, J. C., Dorrell, W., Behrens, T. E., Ganguli, S., and El-Gaby, M. A tale of two algorithms: Structured slots explain prefrontal sequence memory and are unified with hippocampal cognitive maps. *Neuron*, 113(2):321–333.e6, Jan 2025. ISSN 0896-6273. doi: 10.1016/j.neuron.2024.10.017. URL <https://doi.org/10.1016/j.neuron.2024.10.017>.
- Whittington, J. C. R., Dorrell, W., Ganguli, S., and Behrens, T. E. J. Disentanglement with biological constraints: A theory of functional cell types, 2023. URL <https://arxiv.org/abs/2210.01768>.
- Zhang, X., Li, J., Chu, W., Hai, J., Xu, R., Yang, Y., Guan, S., Xu, J., and Cui, P. On the out-of-distribution generalization of multimodal large language models, 2024. URL <https://arxiv.org/abs/2402.06599>.

Zhu, J., Wang, P., Cai, R., Lee, J. D., Li, P., and Wang, Z. Rethinking addressing in language models via contextualized equivariant positional encoding, 2025. URL <https://arxiv.org/abs/2501.00712>.

Zhu, L., Liao, B., Zhang, Q., Wang, X., Liu, W., and Wang, X. Vision mamba: Efficient visual representation learning with bidirectional state space model, 2024. URL <https://arxiv.org/abs/2401.09417>.

## A. Appendix

### A.1. Action-Dependent Matrices Form a Lie Group

The key idea to learn a cognitive map is to move beyond fixed matrices and learn action-dependent matrices, specific to each input action. In (Dorrell et al., 2023), the authors introduce *actionable representations* using group and representation theory, as a formalism to map an input action  $a \in \mathbb{R}^r$  (e.g. in 2D,  $r = 2$  and ‘move right’) to a neural transformation  $W_a \in M_n(\mathbb{R})$  (e.g., the corresponding weight matrix of a neural network that implements the effect of this action on the represented position in space  $p$ ):

$$\begin{aligned} \phi : \mathbb{R}^r &\rightarrow M_n(\mathbb{R}) \\ a &\mapsto W_a \end{aligned} \quad (3)$$

where  $\phi_a$  acts on the representation  $p \in \mathbb{R}^n$  (e.g., abstract position in space) such that  $p(x + a) = W_a p(x)$ . We refer to the matrices  $W_a$ ’s as action-dependent matrices, since unlike standard RNNs, the weight matrix may depend on the specific action taken. To be useful for updating positions in cognitive maps, the action-dependent matrices need to form a group, and specifically, in addition to (1) closure and (2) associativity, it needs to satisfy the following properties: (3) include a matrix for the null action:  $W_0 = \mathbf{I}_n$ , (4)  $\forall a : W_a$  is invertible with inverse  $W_{-a}$  (e.g., ‘one step right’ has the exact opposite effect on the neural representation of ‘one step left’ -  $\forall x, a : p(x + a - a) = W_{-a} W_a p(x) = p(x)$ ). In summary, the requirements for a neural representation for a cognitive map to be consistently and reversibly updated by actions (including a null action and an inverse for every action) mean that the set of action matrices  $\{W_a\}$  must constitute a subgroup of the General Linear Group,  $GL(n, \mathbb{R})$ , under matrix multiplication. Note that this results in various desired properties, such as making the actions  $a$ ’s invariant with respect to the specific position  $p$  they update – In the absence of noise, the action has the same effect on any of the represented positions. Indeed, making the same step right should update the position in the same way whether we are in Paris or New York.

The insight that action-dependent matrices need to form a group, and in particular a Lie group over  $\mathbb{R}$ , allows the use of results from group and representation theory to understand what are the possible constraints on the form of  $W_a$ ’s (Dorrell et al., 2023). Specifically, the Peter–Weyl theorem (Knapp & Knapp, 1996) states that any compact group  $\mathbf{G}$  can be represented in  $M_n(\mathbb{R})$  as:

$$W_a = M \begin{bmatrix} I_1(a) & 0 & \cdots & 0 \\ 0 & I_2(a) & \cdots & 0 \\ \vdots & \vdots & \ddots & \vdots \\ 0 & 0 & \cdots & I_d(a) \end{bmatrix} M^{-1} \quad (4)$$

where  $I_k$  are called the *irreducible representations (irreps)* of group  $\mathbf{G}$  and  $M$  is an invertible matrix. This representation of action-dependent matrices, through the irreps of the group  $\mathbf{G}$ , provides insights into which core actions can be performed by  $W_a$ ’s. For example, for navigation on a circle (1D) or torus (2D), the *irreps* are rotations  $R_{\theta_k}$ :

$$I_k(a) := R_{\theta_k} = \begin{bmatrix} \cos(\omega_k \cdot \Delta_{t_k}) & -\sin(\omega_k \cdot \Delta_{t_k}) \\ \sin(\omega_k \cdot \Delta_{t_k}) & \cos(\omega_k \cdot \Delta_{t_k}) \end{bmatrix}; \quad \theta_k = \omega_k \cdot \Delta_{t_k} \in \mathbb{R}, \quad (5)$$

where  $\omega_k, \Delta_{t_k} \in \mathbb{R}^r, r = 1, 2$  are the angular frequencies and rotation duration, respectively, the former representing movement at different scales. That is, in this example, each  $I_k$  performs a rotation of a subspace of the neural space. The matrix  $M$  then performs a change of basis on this result, assuming  $M$  is not the identity.

### A.2. Path Integration Can Be More Easily Computed in the Lie-Algebra Space

To learn a cognitive map, we saw that it is desirable to require action-dependent matrices to form a Lie group  $\mathbf{G}$ . A Lie group is a group  $G$  that is also a smooth manifold, such that the group operations (multiplication and inversion) are smooth maps. For example, the group of 2D rotations  $SO(2)$  is a Lie group. To build a neural model that can learn cognitive maps, the goal would be to learn action-dependent matrices that form a Lie group.

To further characterize the group of action-dependent matrices, it is often simpler to analyze the corresponding Lie algebra. The associated Lie algebra  $\mathfrak{g}$  of a Lie group  $\mathbf{G}$  is the tangent vector space of  $\mathbf{G}$  at the identity element. Lie-group theory shows the existence of an exponential map between the Lie algebra and the group  $\exp(\cdot) : \mathfrak{g} \rightarrow \mathbf{G}$ , and in the case of a compact group, where the exponential map is surjective, any element  $W_a \in \mathbf{G}$  of the group can be expressed as the exponential of an algebra element  $A$ ,  $W_a = \exp(A) \in \mathbf{G}$ . This is useful since studying the structure of Lie groups (which involves, e.g., matrix multiplication) is often simpler from the point of view of the corresponding Lie algebra (which involves addition operations).

For the case of cognitive maps, we will think of elements of the Lie algebra  $A$ 's as action representations, and the corresponding group elements (expressed via the exponential map) as the action-dependent matrices  $W_a$ 's, which implement these actions in synaptic weights. The exponential map provides the link between the vector space of actions (the Lie algebra) and the space of weight matrices (the Lie group). Specifically, given the property of the exponential map (if the  $A_i$ 's commute, see sec. B.2 for further details):  $\exp(\sum_i A_i) = \prod_i \exp(A_i)$ , the exponential mapping translates the additive structure of the Lie algebra (cumulation of actions in this vector space - e.g, 'move right' then 'move up') into the multiplicative structure of the Lie group (multiplication of the corresponding action-dependent weight matrices). This is useful for path integration, since the cumulative effect of taking actions  $A_1, \dots, A_n$  can be translated to the final action-dependent weight matrix  $W_a = \prod_{i=1}^n \exp(A_i)$ . As we will see, the exponential map allows in some cases to compute path integration in parallel, in the vector space of the Lie algebra, by first computing the cumulative summation of subsequent actions and only then computing the exponent of the result.

For example, for spatial problems, such as navigation on a circle or a torus—and more generally, any 1-dimensional compact group, the Lie group of interest is  $SO(2)$  - the group of all 2D-rotations.

$$R_\theta := \begin{bmatrix} \cos(\theta) & -\sin(\theta) \\ \sin(\theta) & \cos(\theta) \end{bmatrix} \quad (6)$$

The corresponding Lie algebra of  $SO(2)$ , denoted  $\mathfrak{so}(2)$ , consists of all  $2 \times 2$  real matrices  $A$  that are skew-symmetric ( $A^\top = -A$ ). The Lie algebra  $\mathfrak{so}(2)$  is a one-dimensional vector space, spanned by a single basis *skew-symmetric* matrix  $S := -S^\top$  (2D-rotations have a single degree of freedom). Thus, all elements of the Lie algebra can be expressed by a single scalar (the angular velocity)  $\omega$  as  $A = \omega S$ . A finite rotation  $R_\theta$  can then be seen as generated by integrating the infinitesimal angular velocities  $\omega$  over a duration  $\Delta_t$ :

$$S = -S^\top = \begin{bmatrix} 0 & -1 \\ 1 & 0 \end{bmatrix}; R_\theta = \exp(\Delta_t A) = \exp((\omega \Delta_t) S) = \begin{bmatrix} \cos(\omega \Delta_t) & -\sin(\omega \Delta_t) \\ \sin(\omega \Delta_t) & \cos(\omega \Delta_t) \end{bmatrix} \quad (7)$$

Intuitively, the skew-symmetric matrix  $A = \omega S$  defines the instantaneous action direction  $S$  and constant angular velocity  $\omega$ . The finite rotation  $R_\theta \in SO(2)$  is obtained by the exponential map, which performs a continuous integration of this velocity. Thus, the expression  $R_\theta = \exp(\Delta_t A)$  shows that the final rotation yields a total angle of  $\theta = \omega \Delta_t$ , which defines the smooth path (geodesic) on the group manifold.

This framework has important implications for learning a cognitive map. Given that all elements of a compact and connected Lie group (the action-dependent matrices in our case, like rotation groups) can be expressed by the exponential of a single linear combination of the associated Lie algebra generators, learning a cognitive map can be simplified: learning can be performed *at the level of the algebra* rather than the non-linear group level. The algebra primarily involves linear operations and summation – which are naturally compatible with modern deep learning frameworks and backpropagation – while the Lie group involves matrix multiplication. This linearization is useful because the linear path integration required by the exponential map can be much more easily parallelized, as we will see further below.

More generally, given the group of action-dependent matrices  $W_a$ 's (which, as we saw, needs to be a subgroup of the general linear group  $GL(n, \mathbb{R})$ ), elements of the algebra,  $A(t)$ , can be expressed by a linear combination of generators  $A_i$ 's scaled by parameters  $t_i$ 's (the 'integration times', which can be seen as coordinates along the different directions defined by the generators). If surjective, all group elements  $W_a$ 's can then be expressed using the exponential map (fig.2):

$$\begin{aligned}
 A(t) &= \sum_{i=1}^D t_i A_i \in \mathfrak{g}, \quad t_i \in \mathbb{R} \quad (\text{Linear combination in the Algebra}) \\
 W_a &= \exp\left(\sum_{i=1}^D t_i A_i\right) \in G \quad (\text{Mapped to the Group via Exponential})
 \end{aligned} \tag{8}$$

For the special case where the generators  $A_i$  commute (i.e., the Lie bracket is zero), as in the simple  $\text{SO}(2)$  example, the exponential of the sum equals the product of the exponentials:  $W_a = \prod_{i=1}^K \exp(t_i A_i)$ . This shows again the benefit of the Lie algebra: it transforms the non-linear composition (multiplication) of the group into linear path integration (addition) within the algebra, thereby facilitating efficient learning and parallelization in the model.

### A.3. MAmPa: Learning Cognitive Maps with block-diagonal Mamba Models

In this section, we propose a Lie-theoretic interpretation of State-Space Models (SSMs), which provides an interpretation of modern SSMs as models that implicitly perform path integration and can thus learn cognitive maps under certain conditions. This framework reveals a substantial limitation of current state-of-the-art SSMs, such as Mamba and Mamba2 (Gu & Dao, 2024; Dao & Gu, 2024), to meet these conditions for learning cognitive maps. We thus propose a simple modification of the Mamba architecture, which we call **MAmPa**, for learning cognitive **Maps** with **Mamba** models. The link established in (Dao & Gu, 2024) between SSMs and Transformers is what will later allow us to understand the links between absolute and relative positional encoding with models of episodic and working memory, respectively.

Recently, structured state-space models (S4) (Gu et al., 2022) have gained popularity over Transformers as they allow parallelized training of sequences while keeping a linear inference cost. These models are inspired by continuous state space models, where a continuous signal  $x(t) \in \mathbb{R}$  is mapped to  $y(t) \in \mathbb{R}$  via a hidden variable  $h \in \mathbb{R}^n$ :

$$\begin{aligned}
 h'(t) &= Ah(t) + Bx(t) \\
 y(t) &= Ch(t)
 \end{aligned} \tag{9}$$

These continuous systems can be applied to a sequence of discrete tokens, using the zero-order hold (ZOH) rule, which assumes that the input signal  $x(t)$  is constant during a step size  $\Delta$ . This yields the corresponding discrete version of the dynamics:

$$\begin{aligned}
 h_{t+1} &= \bar{A}h_t + \bar{B}x_{t+1} \\
 y_{t+1} &= Ch_{t+1}
 \end{aligned} \tag{10}$$

where  $\bar{A} = \exp(\Delta \cdot A)$  and  $\bar{B} = (\Delta \cdot A)^{-1} (\exp(\Delta \cdot A) - I) \Delta B$ . **This discretization step is fundamental**, as it explains how the exponential map can arise from the integration of infinitesimal recurrent transformations over a time interval  $\Delta \in \mathbb{R}$ . The fact that recurrent computations are defined with a single synaptic weight matrix  $A$  implies that this exponential map can only generate 1-dimensional Lie-algebras, hence commutative groups.

In Mamba, an improved version of (S4), input selectivity is ensured via a per-token learnable step  $\Delta_t$  and matrix  $A$ , that when combined defines a per-token transformation:

$$\bar{A}_t := \exp(\Delta_t A) \tag{11}$$

The exponential relationship between  $A$  (the continuous domain matrix) and  $\bar{A}$  (the discrete domain matrix) directly parallels the relationship between the element  $A$  of the Lie algebra and the weight matrix  $W_a$  in the corresponding Lie group. In the rotation example, since the Lie-algebra  $\mathfrak{so}(2)$  of *skew-symmetric* matrices gives rise to the Lie-group of rotation matrices  $\text{SO}(2)$ ,  $A := \omega S$  is the infinitesimal generator and  $W_a$  is the finite rotation over duration  $\Delta_t$ :  $W_a = \exp(\Delta_t A)$ . By identifying the discrete-time SSM matrix  $\bar{A}$  with the action-dependent matrix  $W_a$ , we propose a new theoretical framework to analyze the capacity of Mamba to learn action-dependent matrices and cognitive maps. In this framework, Mamba can be interpreted as learning action-dependent matrices  $\bar{A}_t$ , which are dynamically created via an exponential map. As we

saw, the exponential map integrates infinitesimal steps via  $A$  (the direction and velocity in the Lie algebra space) over a varying time interval  $\Delta_t$ , giving a finite transformation  $\bar{A}$  (the element of the Lie group). In other words, Mamba implicitly computes *path integration* of action  $A$  over a duration defined by the learned parameter  $\Delta_t$ .

Given this theoretical framework, it is evident that current versions of Mamba are incapable of learning cognitive maps that require, for example, learning rotations. In Mamba,  $A$  was chosen as diagonal, to reduce computational cost, but a diagonal action-dependent matrix cannot learn rotations. This is since  $\bar{A}$  needs to be similar to a block-diagonal matrix, with blocks of size 2 (eq. 4 & 5). Mamba was shown to be able to learn gating problems, which increases the performance of Mamba on various structure-dependent tasks by ignoring irrelevant information, however, Mamba with a diagonal constraint is not expressive enough to represent spatial cognitive maps as Lie-group theory shows. In this work, we modify  $A$  in Mamba to be block-diagonal and, in particular, to blocks of size 2 (for learning rotations) and show that this modification increases the capacity of the model to learn cognitive maps.

#### A.4. MAmPa as a Model of Episodic Memory (EM) and Working Memory (WM)

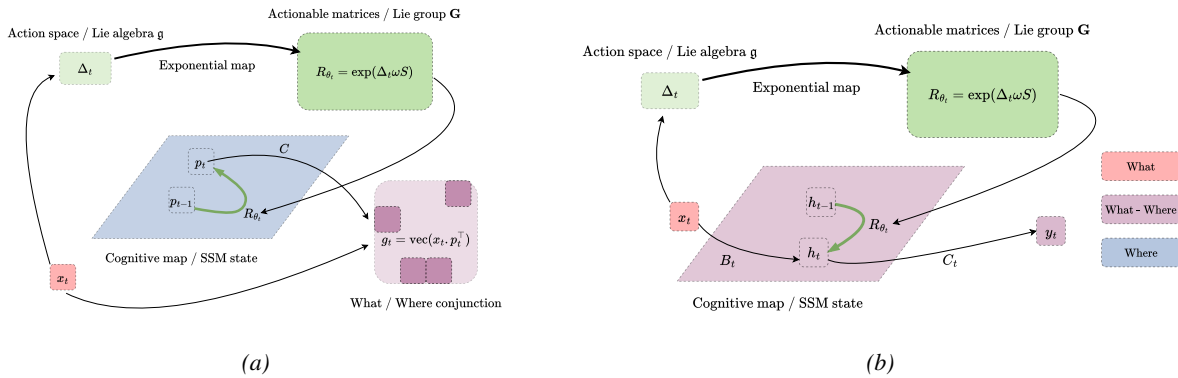


**Figure 5. An illustration of the conceptual framework of action-dependent matrices, and the differences between Episodic Memory (EM) and Working Memory (WM) models (Whittington et al., 2025).** (a) **Episodic Memory (EM) model:** Positions (or ‘states’, more generally) in a cognitive map  $p_t$ ’s (in blue), at times  $t$ ’s, are encoded in a separate neural space by a dedicated neural population, which does not directly interact with the input  $x_t$  (red), being updated via actions only. Actions  $a_t$ ’s, when they occur in the input, can update the position via input-dependent matrices  $W_{a_t}$  (green):  $p_t = W_{a_t} p_{t-1}$ .  $W_a$ ’s are input-dependent matrices and are computed through an exponential map, which maps between abstract representations of actions  $A_t := \Delta_t \omega S = \theta_t S$  (in the Lie-Algebra) and the corresponding weight matrix  $W_{a_t} := \exp(A_t) = R_{\theta_t}$  (in the corresponding Lie group; section A.2). The exponential mapping is computed based on the integration time  $\Delta_t$  of the action (light green) – roughly, how long the synaptic weights  $S$  need to be applied. Finally, the conjunction (purple) of the content (what) and the structure (where) can be computed. (b) **Working Memory (WM) model:** In contrast to the EM model, which factorizes content (red) and position (blue) in two separate neural spaces, *MapFormers*-WM represent position implicitly. Actions in the WM model directly update the conjunction of what and where (purple). The conjunction states  $h_t$ ’s in the WM model are thus smaller by a quadratic factor compared to the EM model.

In (Whittington et al., 2025), the authors introduce two related models of episodic (EM) and working memory (WM) that both learn cognitive maps using RNNs with *input-dependent* matrices. Here, we explain why selective, discrete State-Space Models (SSMs) can be viewed as EM and WM models. First, note that discrete SSMs can be regarded as RNNs with no activation function. Second, selective SSMs learn *input-dependent* matrices via an exponential map (eq. 10), meaning that their inner state captures the task’s latent structure, as in EM/WM models. Therefore, EM and WM models can naturally be regarded as selective SSMs.

**SSM as a model of episodic memory** The EM-RNN model behaves exactly like TEM (Whittington et al., 2019), factorizing structure and content in two distinct neural populations, but only updates its position with an input-dependent RNN  $p_t := W_{a_t} p_{t-1}$ . It then queries a Hopfield memory module (Ramsauer et al., 2021) with its updated position to retrieve passed observations. The RNN in TEM can be seen as an SSM with subtle differences: (1) it uses no external input, *i.e.*  $\forall t, x_t = 0$ ; (2) a learnable embedding  $p_*$  representing the cognitive map’s *zero coordinate* must be introduced to avoid the state being always null; (3) SSM’s inner state must be projected back to its final state ( $y_t = C h_t$ , eq.10), which implies in this case that the final position  $q_t := C p_t$  can be obtained with an optional learnable projection  $C$ ; (4) as in TEM, the

memory module is queried with the conjunction  $g_t$  of **what** has been seen and **where** it was observed (fig. 2a):

$$\begin{aligned}
 p_t &= \exp(\Delta_t A) p_{t-1} = \exp\left(\omega S \sum_{s=0}^t \Delta_s\right) p_* \\
 q_t &= C p_t = C R_{\theta_{0 \rightarrow t}} p_* \\
 g_t &= \text{vec}(x_t^\top \cdot q_t)
 \end{aligned}
 \tag{12}$$

Setting  $C := \mathbf{1}_n$  implies that  $q_t = p_t$ , which is analogous to TEM/EM RNNs. Moreover, compared to RNN based models, this formulation allows to compute path integration directly in the Lie algebra ( $\omega S \sum_0^t \Delta_s$ ) and avoid sequential matrix multiplication.

**SSM as a model of working memory** WM-RNNs directly updates the internal state with input-dependent matrices, which is precisely what selective SSMs do. As such, current selective SSMs with the appropriate matrix structure (*skew-symmetric* in the case of navigation, eq. 5) naturally model working memory (fig. 2b).

Together, this allows us to view SSMs as both EM and WM models, where *the inner state of an SSM can be interpreted as a cognitive map*.

In the previous section, analyzing SSMs through Lie-group theory has allowed us to understand their current limitations, and that one only needs to switch to block-diagonal matrices to theoretically be able to learn a cognitive map. However, previous work decided to keep diagonal matrices because it dramatically reduces the computational load. By treating  $A$  as a vector, one can avoid computing a matrix exponential and also dramatically reduce the memory footprint of a parallel scan, by computing vector-vector multiplications instead of matrix-vector’s. In Mamba2 (Dao & Gu, 2024), it was further reduced to a scalar  $A := a \in \mathbb{R}$ , which allows them to implement a fully parallelized version of selective SSMs but loses the ability to learn cognitive maps, as we have seen above. This highlights a fatal limitations of parallel-selective SSMs: they can be parallelized at the cost of losing any hope of learning a cognitive map (see sec. A.5 for further details). This is the reason why we decided to move away from SSMs and adapt Transformers to learn cognitive maps, as models of episodic (*MapFormer-EM*) and working memory (*MapFormer-WM*).

### A.5. MAMPa: Mamba with skew-symmetric block-diagonal matrices

As explained in sec. A.3, one only needs to modify the recurrent matrix  $A := S = -S^\top$  of selective SSMs to be block-diagonal skew-symmetric in order to learn spatial cognitive maps. We implemented a parallel scan on square matrices to test if **MAMPa**, an extended version of Mamba with  $2 \times 2$  block-diagonal matrices can learn spatial maps like our theory predicts. Because the parallel scan on square matrices dramatically increases the computational load, we kept the inner state small ( $N = 16$ ) and only trained models on sequences of size  $l = 16$  since we did not take the time to implement a custom parallel scan using the efficient implementation of matrix-vector product for rotations used in RoPE (eq. 16), but we expect it to be highly beneficial to learn cognitive maps at scale with Mamba models. We report the results in tab. 3, where OOD dense and OOD sparse use sequences of size 8 and 32 respectively.

	IID	OOD-d	OOD-s
Mamba	0.42	0.77	0.40
<b>MAMPa</b>	<b>0.74</b>	<b>0.93</b>	<b>0.60</b>
<i>MapWM</i>	<b>1.0</b>	<b>1.0</b>	<b>1.0</b>
<i>MapEM-os</i>	<b>1.0</b>	<b>1.0</b>	<b>1.0</b>
<i>MapEM-s</i>	<b>1.0</b>	<b>1.0</b>	<b>1.0</b>

Table 3. **SSM 2D grid navigation - Accuracy.** As expected, *MaMPa* offers substantial improvements over Mamba, but fails to reach performances a par with *MapFormers*, while being slower.

This confirms that our formalism extends to SSMs, but also shows that what has allowed the scaling of selective SSMs – diagonal matrices to reduce the computational load – is what prevents them from learning cognitive maps.

### A.6. Relationship between MapFormers and MAMPa: Linear MapWM are selective SSMs

In sec. 4.1, we have introduced the exponential map in Transformers (via the rotation matrices) to allow them to build *input-dependent* matrices and learn cognitive maps. The Transformer formalism cannot naturally explain how an exponential map emerges like in SSMs, but in Mamba2 (Dao & Gu, 2024), the authors show that linear transformers (Wang et al., 2020) are actually SSMs. Starting from equation 10:

$$\begin{aligned}
 h_t &= A_t h_{t-1} + B_t x_t \\
 &= A_t \dots A_1 B_0 x_0 + A_t \dots A_2 B_1 x_1 + \dots + A_t A_{t-1} B_{t-2} x_{t-2} + A_t B_{t-1} x_{t-1} + B_t x_t \\
 &= \sum_{s=0}^t A_{s \rightarrow t}^\times B_s x_s; \quad A_{s \rightarrow t}^\times := \prod_{i=s+1}^t A_i
 \end{aligned} \tag{13}$$

after multiplying by  $C_t$ , we get the final equation:

$$\begin{aligned}
 y_t &= \sum_{s=0}^t C_t^T A_{s \rightarrow t}^\times B_s x_s \\
 \Rightarrow y &= Mx; \quad m_{ij} := C_j^T A_j \dots A_{i+1} B_i
 \end{aligned} \tag{14}$$

If we remove the matrices  $A_t$ , the matrix  $M := (m_{ij})$ ;  $m_{ij} = C_j^T B_i := q_j^T k_i$  can be seen as the key-query similarity matrix  $QK^T$  without softmax normalization, as in linear transformers. Equation 14 is fundamental as it characterizes exactly how actionable representations can be implemented in transformers, where matrix  $A_{i \rightarrow j}^\times = A_j \dots A_{i+1}$  represents the model's path integration between tokens  $i$  and  $j$ .

If we choose matrix  $A := S$  to be a  $2 \times 2$  block-diagonal skew-symmetric matrix and  $R_t := \exp(\theta_t S) = \exp(\Delta_t \omega S)$  as in equation 7, we retrieve the definition of RoPE (Su et al., 2023):

$$\begin{aligned}
 m_{ij} &= q_j R_{i \rightarrow j}^\times k_i \\
 &= q_j^T R_{0 \rightarrow j}^\times (R_{0 \rightarrow i}^\times)^{-1} k_i \\
 &= (\bar{R}_j q_j)^T (\bar{R}_i k_i); \quad \bar{R}_i := (R_{0 \rightarrow i}^\times)^{-1} = \exp\left(-\sum_{s=0}^i \Delta_s \omega S\right) := \exp\left(\sum_{s=0}^i \theta_s S\right) \\
 &= \text{RoPE}(q_j, k_j)
 \end{aligned} \tag{15}$$

**This proves that linear RoPE transformers are SSMs with a  $2 \times 2$  skew-symmetric recurrent matrix**, where  $\theta_t$  controls the angle of rotation. In Mamba2, the authors define  $A := a \in \mathbb{R}$  as a scalar, giving  $M_{ij} = \exp(-a \sum_{t=i+1}^j \Delta_t) q_j^T k_i$ , which is analogous to the cumulative gating of CoPE (Contextualized Positional Encoding) (Golovneva et al., 2024), with a multiplicative and not additive binding operation. CoPE is an enhanced Transformer architecture with context-dependent positional encoding, that like Mamba compresses the relative key-query distances with a cumulative gating mechanism, and in both models, input selectivity allows them to focus or ignore certain tokens and solve structure-dependent tasks, but should not allow them to learn spatial cognitive maps.

This extends the unification of transformers with models of episodic memory (EM) started in TEM-t (Whittington et al., 2022), showing that the difference between absolute and relative positional encoding can be better understood via the SSM formulation. EM models use *action-dependent* matrices on a dedicated neural population (absolute positional encoding), before querying an external memory module, *i.e.* modeling memories in synaptic activity, while WM models directly update the whole neural activity with *action-dependent* matrices, directly

### A.7. Implementation details

We chose rotation matrices because they are well suited to represent most bounded commutative structures (like movement on a finite grid or integers modulo  $N$ ), but also because they have useful numerical properties: (1) rotations and their inverse are orthogonal and therefore ensure numerical stability, not present in Mamba, since the inverse of the exponential gating

matrix they use diverges towards infinity, making it impossible to represent both an action and its inverse in a numerically stable way; (2) their transpose is also their inverse, implying that the key-query dot product  $\bar{q}_j^\top \cdot \bar{k}_i = q_j^\top R_{PI_{i \rightarrow j}} k_i$  represents path integration between tokens  $i$  and  $j$ , necessary to learn cognitive maps in parallel.

Rotations can be ensured by enforcing  $S := \bar{S} - \bar{S}^\top$  to be skew-symmetric, but since a single generator matrix  $S$  can only generate rotations along a single axis (see sec.B.2.2 for further details), choosing blocks of size  $b > 2$  is useless as it increases the computational load while effectively reducing the amount of rotations being performed. Using blocks of size 2 also allows us to use the explicit *irreps* representation of  $2 \times 2$  rotations and avoid computing a matrix exponential (eq.5). This also allows, as in RoPE (Su et al., 2023), to rewrite matrix multiplication of  $R_\theta x$  in *MapFormers* as:

$$R_\theta x = \begin{pmatrix} x_1 \\ x_2 \\ \vdots \\ x_{d_h-1} \\ x_{d_h} \end{pmatrix} \odot \begin{pmatrix} \cos(\Delta_{t_1} \cdot \omega_1) \\ \cos(\Delta_{t_1} \cdot \omega_1) \\ \vdots \\ \cos(\Delta_{t_{n_b}} \cdot \omega_{n_b}) \\ \cos(\Delta_{t_{n_b}} \cdot \omega_{n_b}) \end{pmatrix} + \begin{pmatrix} -x_1 \\ x_2 \\ \vdots \\ -x_{d_h-1} \\ +x_{d_h} \end{pmatrix} \odot \begin{pmatrix} \sin(\Delta_{t_1} \cdot \omega_1) \\ \sin(\Delta_{t_1} \cdot \omega_1) \\ \vdots \\ \sin(\Delta_{t_{n_b}} \cdot \omega_{n_b}) \\ \sin(\Delta_{t_{n_b}} \cdot \omega_{n_b}) \end{pmatrix} \quad (16)$$

leaving only angular velocities  $\omega \in \mathbb{R}^{n_b}$  (see sec. A.8 for a discussion about their initialization) as learnable parameters instead of matrix  $S \in \mathbb{R}^{n_b \times b \times b}$ .

The actual rotation angle  $\theta_t = \omega \Delta_t$  is dynamically computed from the input features  $X$  using a low-rank projection  $W_\Delta = W_\Delta^{out} W_\Delta^{in}$ . The goal of this two-step process is to ensure the rotation relies only on the most salient action features of the input. First, the internal projection  $W_\Delta^{in} \in \mathbb{R}^{d \times r}$  ( $r \ll d$ ) maps the high-dimensional input  $X$  to a low-dimensional  $\Delta_t^{in} \in \mathbb{R}^{t \times r}$  (for instance, in a 2D environment,  $\Delta_t^{in}$  could be the 2D movement vector  $\Delta_{t_k} \in \mathbb{R}^r$  in eq. 5, where  $r = 2$ ). Second, this extracted action is projected by  $W_\Delta^{out}$  into the final set of path increments  $\Delta_t \in \mathbb{R}^{t \times n_h \times n_b}$ , which controls the rotation angle for all attention heads ( $n_h$ ) and all diagonal blocks ( $n_b$ ), where  $n_b = d_h/b$  is the number of blocks per head dimension.

Finally, compared to TEM and TEM-t that use a single neural population  $p_t$  to encode position, our *MapFormers* use two separate initial vectors  $k_0^p$  and  $q_0^p$ . This distinction is optional and mimics the formalism of EM-SSMs defined in eq. 12, meaning that we could set  $k_0^p = q_0^p = p_0$  without loss of generality. However, we suspect this separation to be beneficial because it would create sparser attention values. Indeed, our positions  $p_t$  vary smoothly through path-integration, implying that nearby positions would not be strongly separated, but introducing distinct neural populations for keys and queries could allow the model to find the optimal balance between separation/matching of distinct/similar positions.

Recall that the conjunctive query  $g_i^q := \text{vec}(q_j^{x^\top} \cdot q_i^p)$ , the conjunction of what has been seen and where. Since  $\forall i, j : \langle g_i^q, g_j^k \rangle = \langle q_j^{x^\top} \cdot q_i^p, k_i^{x^\top} \cdot k_j^p \rangle = \langle q_j^x, k_j^x \rangle \langle q_i^p, k_i^p \rangle$ , we can avoid the outer products  $Q_X^\top Q_P$  and  $K_X^\top K_P$  by computing content and position attentions  $A_X = \text{Att}(Q_X, K_X)$  and  $A_P = \text{Att}(Q_P, K_P)$  separately (still in parallel by concatenating the heads), such that  $A_P$  acts as an attention mask on  $A_X$

The fact that *MapFormer*-EM models rely on observations (content) or structure (position) attention  $A_X$  and  $A_P$ , allows to balance between the two attention maps to compute similarities. To test the impact of each modality, we introduce three types of EM models: (1) *MapEM*-os relying on both observation and structure to compute attention; (2) *MapEM*-s relying on structure alone and (3) *MapEM*-o relying solely on observation, equivalent to a Transformer without positional embeddings, serving as a control. Note that ideally, the model should learn to balance between observation or structure depending on context, but we decided to leave it for future work. This forced separation is primarily used to highlight the benefits of focusing on different modalities depending on the task.

### A.8. Angular velocities initialization

Like *grid cells* that fire at different frequencies (Hafting et al., 2005), our formalisms uses rotations at different scales, scale whose initialization has a major impact on position representations.

The highest angular velocity (or frequency  $f$ , assuming  $\omega = 2\pi f$ )  $\omega_{max}$  defines the finest granularity  $\Delta_{min} = \frac{2\pi}{\omega_{max}}$  at which the signal is encoded, while low frequencies encode long range dependencies. We would like the lowest angular velocity  $\omega_{min} := \frac{2\pi}{\Delta_{max}}$  to complete its cycle once the the model has covered the longest distance  $\Delta_{max}$  it possibly can, where  $\Delta_{max} = n$  on a  $n$ -size grid (fig. 6).

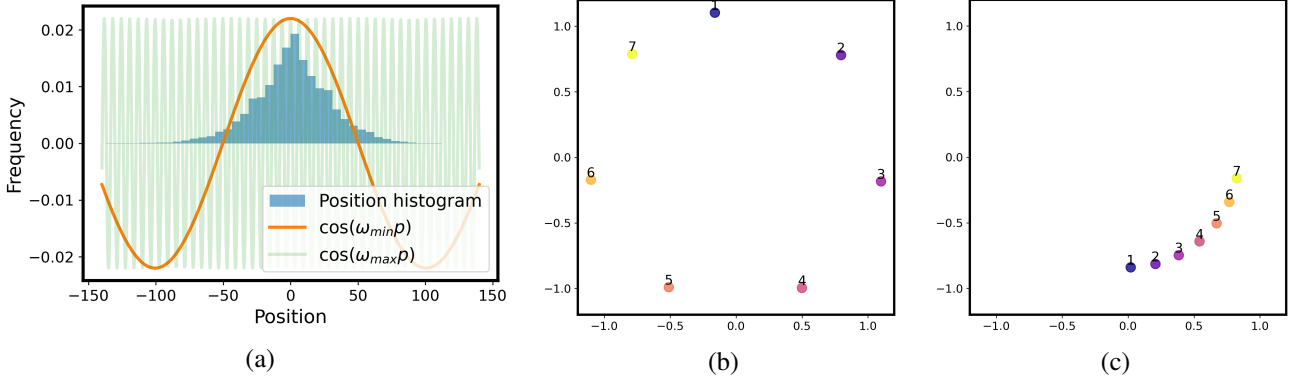


Figure 6. (a) Distribution histogram of position in 1D navigation vs oscillation at the highest (green) and lowest (orange) angular velocities. The longest distances reached by the model are comparable with the length of  $\omega_{min}$  cycles. (b-c) Rotation blocks at high and low frequencies.

Angular velocities should encode signal at different scales, and a geometric initialization like the one used in RoPE (Su et al., 2023) spreads the scales uniformly between 1 and  $\Delta_{min} = \frac{1}{base}$  with:

$$\omega_i = \left( \frac{1}{\Delta_{max}} \right)^{-\frac{i}{n_b}}, \quad 1 \leq i \leq n_b$$

where  $base \approx 10000$  in RoPE, dictates how many tokens the model has to see before completing a full circle. Compared to RoPE that always rotates by a constant rotation duration  $\Delta = 1$ , our input-dependent rotation durations  $\Delta_t$  can take values below 1, and as such we might want our highest angular velocity  $\omega_{max}$  to be greater than 1. We extend the logic such that:

$$\forall i : \omega_i = \omega_{max} \left( \frac{1}{\Delta_{max}} \right)^{-\frac{i}{n_b}} \implies \begin{cases} \omega_{max} = \frac{2\pi}{\Delta_{min}} \\ \omega_{min} = \frac{\omega_{max}}{\Delta_{max}} = \frac{2\pi}{n} \\ \implies \Delta_{max} = \frac{n \times \omega_{max}}{2\pi} \end{cases} \quad (17)$$

Leaving only  $\omega_{max}$  and  $base := n$  as hyperparameter-parameters and find that initializing  $1 < \omega_{max} \leq 2\pi$  to work well in practice.

## B. Further experiments and methods

When generating trajectories, to favor grid exploration, we uniformly sample a direction and the number of steps  $k$  to pursue in that direction ( $1 \leq k \leq 10$ ). Otherwise, agents would be statistically stuck in small environments.

For 1D/2D grid navigation, we trained all models on sequences of  $l = 128$  steps, a grid size of  $l_{grid} = 64$ , and a probability of placing an object at a specific location  $p_{empty} = 0.5$ . We tested length generalization on two OOD datasets - OOD-d:  $l = 64, p_{empty} = 0.2, l_{grid} = 32$  and OOD-s:  $l = 512, p_{empty} = 0.8, l_{grid} = 128$ .

Unless stated otherwise, for 1D-2D navigation and beyond, we trained single layer models with two heads of size  $h = 64$  on 200K sequences, with AdamW optimizer (Loshchilov & Hutter, 2019), a linear learning rate decay, a base learning rate  $lr = 3e^{-4}$ , weight decay 0.05 and a batch size of 128 on a single GPU.

### B.1. 3D and 5D navigation

Because translations in  $n$  dimensions are just  $n$  independent 1D-translations on orthogonal axes, our models should theoretically be able to track position on these structures – with rotation blocks representing movement on one specific dimension – but should require a higher number of neurons to represent movement on all these orthogonal axes.

We train all models with a head size of 64. In 3D, we choose a sequence length of 256 and a grid size of 16. The task being particularly hard in 5D, we decided to reduce the sequence length to 16 and the grid size to 5 and report the results in tab. 4.

	3D navigation			5D Navigation		
	IID	OOD-d	OOD-s	IID	OOD-d	OOD-s
RoPE (1L)	0.39	0.36	0.35	0.74	0.45	0.33
CoPE (1L)	0.78	0.82	0.74	0.94	0.80	0.69
<b>MapWM</b>	<b>1.0</b>	0.95	0.94	0.75	0.50	0.35
<b>MapEM-os</b>	<b>1.0</b>	<b>0.99</b>	<b>0.99</b>	<b>1.0</b>	<b>0.98</b>	<b>0.84</b>
<b>MapEM-s</b>	<b>1.0</b>	<b>1.0</b>	<b>0.98</b>	<b>1.0</b>	<b>1.0</b>	<b>0.87</b>

Table 4. **3D - 5D grid navigation accuracy.**  $2 \times 2$  block-diagonal rotation matrices can represent translations in 3D and 5D, since it equivalent to (3 or 5) 1D orthogonal translations. However, performances quickly degrade, since the amount of positions to represent grows exponentially. Notably, in 5D, *MapWM* fails to learn the task and perform a par with RoPE, while *MapEM*, which scale better in recall tasks, solve it even though performances start to degrade on longer sequences.

As we can see, all of our models converge in dimension 3, confirming that 2D-rotations are enough to learn simple translations in higher dimension. However, our WM models never manage to learn a cognitive map in 5D, and actually performances comparable to RoPE and much worse than CoPE, showing once again the increased robustness of EM models on recall tasks. Note that in 5D, because we keep the world size and sequence length small, CoPE asymptotically approaches a perfect score on the training set but fails to generalize OOD, while EM models solve it with 6 times less training data and generalize, highlighting the difference between learning of a cognitive map versus statistical heuristics. Models learning a cognitive map achieve robust generalization with much fewer data points, something that has been observed when comparing learning efficiency in humans versus AI models.

### B.2. Non-commutative groups

So far, all our experiments were run with  $2 \times 2$  block-diagonal matrices, which we demonstrated in section B.1 to be enough to capture translations in higher dimensions, as rotations on orthogonal circles. However, it is unlikely that the brain performs perfect rotations, and a model should be able to converge to the desired matrix representation. In this section, we decided to explore matrices beyond  $2 \times 2$  rotations, and analyze the tradeoff between model’s expressivity and inference speed. We will start by analyzing the impact of increasing the block size of our rotation matrices, as well as changing their structure, to not be skew-symmetric anymore. Finally, we will analyze non-commutative group structures, and show that they can be learned, at the cost of losing parallel sequence abilities.

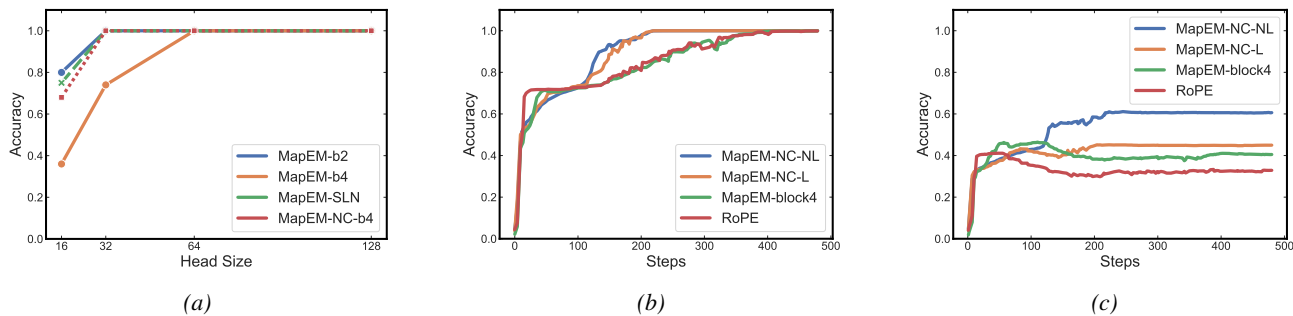


Figure 7. **Influence of matrix structure, block size and non-commutativity on the ability to learn cognitive maps.** (a) All models were trained on sequences of length 128. *MapEM* performances drop significantly when varying block size from 2 (blue) to 4 (orange) since it reduces the amount of learned rotations. Having a non commutative model of size 4 (red) allows to flexibly switch between rotations on each blocks, and keep performances competitive with blocks 2. Other group structures like  $SL(2, n)$  can also be used (*MapEM-SLN*, green). (b-c) Navigation on 4D-rotations, needing non commutative matrices. We introduce *MapEM-NC-L* and *MapEM-NC-NL*, two non commutative variants of EM models, where  $\theta_i$  are learned respectively via linear and non-linear functions. (c) Accuracy through training, where non-commutative reach a perfect accuracy early, while EM and RoPE approach it asymptotically. (d) Generalization to double sequence length. Only NC-NL manages not to drop in accuracy, showing the difficulty of learning a non-linear Lie algebra  $\mathfrak{g}$

### B.2.1. OTHER COMMUTATIVE GROUPS

The first experiment that we conducted was to increase the block size of our rotation matrices. Since a single generator matrix  $S$  can only generate rotations along a single axis, we anticipate that using blocks of size  $b > 2$  should be useless since it requires more neurons to perform a similar operation, and cannot benefit from the explicit formulation of matrix exponential (eq 4). It is what we observe in fig.7a, where *MapEM*-b4, EM model with blocks of size  $b = 4$  (orange), needs twice the amount of neurons than *MapEM*-b2 (blue).

Aside from block size, as Lie-group theory predicts, the nature of matrix  $A$  influences the learned structure. The special linear group  $SL(n, \mathbb{R})$  – which preserves determinant, *i.e.* areas – can be represented using matrices with a null trace:  $A = \bar{A} - \text{Tr}(\bar{A}) \implies \text{Tr}(A) = 0$ . This group is more expressive than  $SO(n)$  (but not compact), and we show that it can also be used to solve navigation tasks (fig. 7a, *MapEM*-SLN, block-size 2, green).

Finally, we tested *MapEM*-NC, a non-commutative model that we detail further in sec. B.2.2. This model learns a basis of rotations per block  $S_i, 1 \leq i \leq K$ , allowing it to switch rotation axes on the fly. We show that such a model with block size  $b = 4$  and basis size  $K = 6$  (red) performs a par with *MapEM*-b2, and much better than a model with the same block size but a single generator matrix  $S$  (*MapEM*-b4). This implies that what matters is the amount of rotations to perform rather than the block size in itself.

### B.2.2. NON COMMUTATIVE LIE GROUPS

The ability to learn non commutative rules is fundamental, since rules as simple as "mother" and "father" should not commute. Indeed, the father of my mother is my grand father on my mother's side, while the mother of my father is my grand mother on my father's side, hence ending in a different position within the family tree/graph. This implies that the learned matrices do not commute, *i.e.*:  $\mathbf{W}_{mother} \mathbf{W}_{father} \neq \mathbf{W}_{father} \mathbf{W}_{mother}$ .

Compared to dimension 2 where a single  $2 \times 2$  skew-symmetric matrix  $S$  is enough to generate any rotation, the basis of skew-symmetric matrices scales quadratically, since there are  $n(n-1)/2$  ways to permute axis in dimension  $n$ , meaning that a single weight matrix will never be enough to encode all these rotation axis. Therefore, any rotation in  $SO(n)$  must be expressed with a basis of  $n(n-1)/2$  skew-symmetric matrices  $\{S_i\}_{1 \leq i \leq K}$ , matrices that do not commute together in general ( $S_i S_j \neq S_j S_i$ ):

$$R_\theta^n = \exp \left( \sum_{i=1}^{n(n-1)/2} \theta_i S_i \right) \neq \prod_{i=1}^{n(n-1)/2} \exp(\theta_i S_i) \quad (18)$$

We see here that non-commutativity implies that path integration cannot be performed via the exponential of a sum anymore and can only be achieved via a sequential matrix product scaling linearly with sequence length  $L$ .

We introduce non-commutative models (NC), with a basis of  $K = n(n-1)/2$  skew-symmetric matrices  $\{S_i\}_{1 \leq i \leq K}$ ,  $\theta := \Delta_t \omega \in \mathbb{R}^{n_h \times n_b \times K}$  and  $R_\theta = \exp \left( \sum_{i=1}^K \theta_i S_i \right)$ . The non commutativity forces us to compute path-integration sequentially and use a parallel scan to speed-up computation, since our models cannot leverage the parallel processing abilities of Transformers anymore, making them analogous to TEM-t (Whittington et al., 2022), where path integration is computed sequentially before computing attention.

When the Lie group  $\mathbf{G}$  is not commutative, the coordinates  $\Delta_t \omega S_i$  do not add-up linearly,  $\mathfrak{g}$  becomes a curved manifold and cannot be treated as a vector space anymore. For that reason, we hypothesize that a linear mapping like we used in our *MapFormer* models should not capture the complexity of the group's manifold. Because of this, we introduce two non-commutative variants. (1) **MapEM-NC-L** with a linear mapping:  $\Delta_t := W_\Delta x_t$  and (2) **MapEM-NC-NL** that uses an MPL to infer the rotation angles  $\Delta_t := f_\Delta(x_t)$ .

To validate our theory, we reproduce our navigation task, where this time actions represent 4D notations and not translations anymore, needing a non-commutative Lie algebra in order to be solved. The task being particularly hard, and our non-commutative models slow to train, we train our models on sequences of length 16, and test on length 32. We compare our models to RoPE and an *MapEM*-s with block size 4 in fig. 7b & 7c. As expected, our two EM-NC model solve the task faster, while EM and RoPE reach a perfect accuracy asymptotically, implying that they probably memorized the training dataset. However, only our non-commutative model with a non-linear mapping (*MapEM*-NC-NL) has non-degrading performances on the OOD dataset (fig 7c, blue), but still far from perfect accuracy. This highlights the importance of learning non-commutative rotations, but also how difficult it is to approximate the curvature of a non-commutative Lie

algebra. Further work should investigate how to improve the computation of rotation angles  $\theta := \omega \Delta_t \in \mathbb{R}^{n(n-1)/2}$ , that clearly has an impact on final performances.